Analytical Biochemistry 435 (2013) 174–180

Contents lists available at SciVerse ScienceDirect

Analytical Biochemistry

journal homepage: www.elsevier.com/locate/yabio

Electroformation of giant unilamellar vesicles from erythrocyte membranes under low-salt conditions

Miha Mikelj [a,1], Tilen Praper [a,1,2], Rok Demič [a], Vesna Hodnik [a], Tom Turk [a], Gregor Anderluh [a,b,*]

[a] Department of Biology, Biotechnical Faculty, University of Ljubljana, 1000 Ljubljana, Slovenia
[b] National Institute of Chemistry, 1000 Ljubljana, Slovenia

ARTICLE INFO

Article history:
Received 29 February 2012
Received in revised form 24 December 2012
Accepted 2 January 2013
Available online 17 January 2013

Keywords:
Electroformation
Giant unilamellar vesicles
Erythrocytes
Protein binding

ABSTRACT

Giant unilamellar vesicles (GUVs) are an attractive experimental model for studying various membrane-related phenomena. The procedure for GUV electroformation from erythrocyte ghosts under physiological conditions was introduced recently; however, it allows preparation of a limited number of GUVs. Here we describe an efficient, reliable, and simple method for electroformation of GUVs from native erythrocyte membranes at low salt concentration, which enables the formation of higher amounts of large, spherical GUVs. GUVs prepared according to the new procedure may not retain original lipid asymmetry; however, they preserved native proteins, lipids, and oligosaccharide heterogeneity and could be a suitable system for functional studies for which larger amounts of GUVs of complex composition are needed.

Giant unilamellar vesicles (GUVs) have become an intensively used model system for studying various processes involving lipid membranes. With diameters up to 100 μm, GUVs have sizes comparable to eukaryotic cells and are well distinguished by commonly used optical methods such as light and fluorescence microscopy [1]. Because of their large size, the vesicles' radii are much greater than the membrane thickness. Consequently, the GUV membranes are practically flat with virtually no curvature at the molecular level [2]. GUVs have significant advantages in comparison to smaller liposomes such as large unilamellar vesicles (LUVs) prepared by extrusion or small unilamellar vesicles (SUVs) prepared by sonication. The average values of the physical parameters of liposomes are obtained from large numbers of liposomes when using LUVs or SUVs and thereby much information may be lost [3]. GUVs have been successfully used as a model system to study fundamental membrane thermodynamics [4], membrane curvature [5], morphology [6], and membrane domains [7]. Since GUVs allow optical measurements at the single-vesicle level while tracking membrane integrity they can also provide novel information about the mechanism of pore formation induced by peptides or proteins [1,8].

There are several techniques for preparing GUVs, e.g., gentle hydration [9], solvent evaporation [10], microfluidic jetting [11], and electroformation [12]. Electroformation is particularly useful and convenient and, therefore, widely used for preparation of GUVs. In this method lipids solubilized in organic solvents, e.g., a mixture of chloroform and methanol, are deposited on the electrode, dried, and then exposed to an AC field [12]. The principle of GUV formation in not well understood. It was proposed that mechanical stress induced by the AC field plays a role in separating and destabilizing the membranes to form liposomes [12]. Electroformation has been reported to succeed only in solutions with ionic strengths below 50 mM [13]. However, recently a new procedure was introduced that allows electroformation in buffers with physiological ionic strength (e.g., at >100 mM KCl or NaCl) [14–16]. The major difference in the novel procedure is in the frequency of the AC field. While classical electroformation procedures involve low frequency (typically ~10 Hz), the novel procedure uses a high-frequency AC field (~500 Hz). Furthermore, the novel procedure enables for the first time the electroformation of GUVs from erythrocyte ghosts, which represent the native lipid deposit [15]. The yield of GUVs gathered from this procedure was rather low and here we developed a new procedure, which improved the efficiency of GUV formation and thus enables a highly concentrated suspension of GUVs to be obtained. The protocol contains a membrane drying step and, therefore, the original lipid asymmetry and functionality of some of the proteins may not be preserved. However, GUVs so obtained have a complex composition and may be useful in functional studies in which larger amounts of GUVs are needed.

* Corresponding author at: National Institute of Chemistry, 1000 Ljubljana, Slovenia. Fax: +386 1 476 03 00.
E-mail address: gregor.anderluh@ki.si (G. Anderluh).
[1] These authors contributed equally to this work.
[2] Present address: Lek Pharmaceuticals d.d., Biopharmaceuticals, 1234 Mengeš, Slovenia.

0003-2697/$ - see front matter © 2013 Elsevier Inc. All rights reserved.
http://dx.doi.org/10.1016/j.ab.2013.01.001

Materials and methods

Materials

1,1′-Dioctadecyl-3,3,3′,3′-tetramethylindodicarbocyanine perchlorate ($DilC_{18}$) was from Invitrogen (Carlsbad, CA, USA). 1-Palmitoyl-2-oleoyl-*sn*-glycero-3-phosphocholine (POPC) was from Avanti Polar Lipids (Alabaster, AL, USA). FITC-labeled anti-glycophorin and anti-perforin monoclonal antibodies were from Santa Cruz (Santa Cruz, CA, USA). Mouse polyclonal anti-A and anti-B antibodies were provided by Dr. Simon Koren (Blood Transfusion Center of Slovenia). Secondary FITC-labeled anti-mouse antibodies were from Imgenex (San Diego, CA, USA). All other chemicals were from Sigma (St. Louis, MO, USA) or Merck (Darmstadt, Germany).

The solution osmolality measured by a freezing-point osmometer (Knauer, Germany) was approximately 300 mOsmol/kg. All buffers used for electroformation and sedimentation were isoosmolal.

Preparation of erythrocyte membranes and ghosts

Blood was collected from a healthy volunteer, placed in EDTA tubes (Vacuette; Greiner Bio-One, Frickenhausen, Germany), and washed with 140 mM NaCl, 5 mM Na_2HPO_4, pH 8.0. Washed erythrocytes were lysed with approximately 40 vol of cold 5 mM Na_2HPO_4, pH 8.0, and incubated 5 min on ice and centrifuged 20 min at 25,000*g* at 4 °C. The last step was repeated several times until all of the hemoglobin was removed from the membrane pellet. For the production of erythrocyte membranes the membrane pellet was separated from the supernatant and washed several times with water at 4 °C. For the production of ghosts, the membranes were washed by buffer containing 150 mM NaCl, 20 mM Hepes, pH 7.4 (protocol 1) or water (protocol 2) and then subjected to 10 freeze–thaw cycles (frozen by liquid nitrogen and thawed in water at 37 °C). Afterward, ghosts were incubated for 2 h at 37 °C. The concentration of membranes and ghosts was adjusted to phospholipid concentration of 0.8 mg/ml. For the fluorescence microscopy experiments, membranes and ghosts were labeled by adding $DilC_{18}$ (1 mg/ml, in dimethyl sulfoxide) to a suspension of membranes or ghosts in a ratio of 1:100 (v/v).

Electroformation

Membranes or ghosts were spread onto a pair of Pt electrodes (dimensions: ϕ: 1 mm, length 34 mm, spacing between electrodes 4 mm) and dried 5 min at atmospheric pressure (ghosts) or under reduced pressure for >2 h (membranes). Electrodes were then placed into a vial filled with 1.4 ml of water (protocol 4) or buffer containing 150 mM NaCl, 20 mM Hepes (protocols 1–3) or sucrose solution containing 295 mM sucrose, 1 mM Hepes (protocols 5 and 6). AC current was applied with a functional generator (GW Instek GFG-3015). Two different electroformation programs were used: a high-frequency (500 Hz) protocol and a low-frequency protocol (10 Hz). The high-frequency protocol for electroformation was performed as follows [15]: 5 min of 140 mV/500 Hz, 20 min of 1.25 V/500 Hz, 90 min of 3.5 V/500 Hz. The low-frequency protocol was performed as follows [17]: 2 h of 4 V/10 Hz, 15 min of 2 V/5 Hz, 15 min of 1 V/2.5 Hz, 30 min of 1 V/1 Hz. Electroformation was performed at 37 °C. Experimental conditions for the individual protocols are summarized in Table 1.

Fluorescence microscopy

Fluorescence and differential interference contrast (DIC) microscopy was performed on an AxioImager Z1 (Carl Zeiss, Germany) equipped with an ApoTome for grid-confocal microscopy (optical sections by ApoTome were recorded for Figs. 4B and 5C) and 100-W HBO mercury arc illumination. Calcein, FITC-labeled dextrans, and antibodies were observed with 450–490 nm bandpass excitation and 515 nm longpass emission filter. The membranes of the red blood cell (RBC)–GUVs containing $DilC_{18}$ were observed with 546/12 nm bandpass excitation and 590 nm longpass emission filter. Six microliters of GUV suspension was mixed with 0.5 μl of fluorescent dextran FD70 or calcein (final concentration of FD70 or calcein was 0.01 mM) for the permeabilization studies. Nine microliters of RBC–GUV suspension was mixed with 0.5 μl FITC-labeled anti-glycophorin and anti-perforin antibodies (both IgG2b isotype, stock c = 0.2 mg/ml) or 1 μl anti-A and anti-B primary antibodies (stock c = 0.1 mg/ml) for the immunodetection studies. The whole suspension was gently mixed by pipette and incubated 20–40 min at 25 °C. Blood group antigens were visualized by adding 0.5 μl FITC-labeled secondary antibody (stock c = 1.4 mg/ml), gently mixed, and incubated at 25 °C for 30 min.

Protein concentration determination

Five hundred microliters of GUV suspension after protocol 2 or 5 was blotted onto nitrocellulose membrane paper using a Minifold dot-blot system (Gentaur, Belgium). Proteins bound to a membrane were stained by amido black as described [18]. Briefly, nitrocellulose-bound proteins were stained for 6–10 min by amido black staining solution containing 0.1% (w/v) amido black, 25% (v/v) isopropanol, 10% (v/v) acetic acid and destained for 5 min in an aqueous solution containing 25% (v/v) isopropanol and 10% (v/v) acetic acid. The protein concentration was calculated from the calibration curves prepared using bovine serum albumin (BSA). For the calculation of proteins after protocol 2, six dilutions of BSA ranging from 0.5 to 50 μg/ml in a buffer containing 150 mM NaCl,

Table 1
Protocols used for electroformation of GUVs

Step	Protocol					
	1	2	3	4	5	6
Lipid deposit						
Material	Ghosts	Ghosts	Membranes	Membranes	Membranes	Membranes
Volume (μl)	16	16	16	16	16	2
Solution	Buffer	Water	Water	Water	Water	Water
Drying						
Time	5 min	5 min	>2 h	>2 h	>2 h	>2 h
Pressure (Pa)	10^5	10^5	5000	5000	5000	5000
Electroformation						
Frequency (Hz)	500	500	500	10	10	10
Solution	Buffer	Buffer	Buffer	Water	Sucrose	Sucrose

A detailed description of each protocol for electroformation is described under Materials and methods.

20 mM Hepes were blotted and stained on the same membrane as the GUV suspension. For the GUVs formed by protocol 5, BSA was diluted in a sucrose solution containing 295 mM sucrose, 1 mM Hepes. The quantification of protein spots on the nitrocellulose membrane was performed densitometrically by ImageJ 1.43 (Java-based image processing open source software).

Cholesterol and phospholipid concentration determination

A half-milliliter of GUV suspension was dried overnight at room temperature by vacuum concentrator (Genevac, USA), to concentrate enough material for the phospholipid and cholesterol analysis. Phospholipid and cholesterol concentration was determined using the Phospholipids C and Free Cholesterol E kits (Wako Diagnostics, USA) according to the manufacturer's instructions.

Enzymatic assays

Acetylcholinesterase (AChE) activity was measured according to the method of Ellman et al. [19] and optimized for microtiter plates (Bio-Tek Instruments, USA; PowerWave XS) by Mancini et al. [20]. Briefly, 10 μl of sample (various membrane preparations—details are described under Surface plasmon resonance, or GUVs prepared using protocol 1 and 5) was added to 90 μl of 100 mM potassium phosphate buffer, pH 7.4. To start the reaction, 100 μl of 2 mM acetylthiocholine iodide in Ellman's reagent was added. Hydrolysis of acetylthiocholine iodide was followed spectrophotometrically at 412 nm at 25 °C for 5 min on a Kinetic Microplate Reader (Dynex Technologies, USA) [20]. AChE activity was expressed in nmol of hydrolyzed acetylcholine chloride/min/mg protein (extinction coefficient $\varepsilon_{412} = 13{,}600\ M^{-1}\ cm^{-1}$). K^+-(*p*-nitrophenyl phosphatase) activity was determined according to the method of Marcheselli et al. [21]. Ten microliters of the sample was added to 240 μl of the assay mixture (50 mM Tris–HCl, 3 mM $MgCl_2$, 10 mM KCl, 3 mM *p*-nitrophenyl phosphate, pH 7.5) and incubated at 37 °C for 1 h. The absorbance at 405 nm was determined after incubation. K^+-(*p*-nitrophenyl phosphatase) activity was expressed in nmol of produced *p*-nitrophenol/min/mg protein (extinction coefficient $\varepsilon_{405} = 18{,}800\ M^{-1}\ cm^{-1}$). Protein concentration was determined by assay with the Bradford reagent (Bio-Rad).

Surface plasmon resonance

The binding of ouabain to various membrane preparations was assessed using surface plasmon resonance (SPR) [22,23]. The erythrocyte membranes were prepared as described above. For preparation of dried and sonicated membranes, membranes were dried under pressure with a miVac Duo centrifugal vacuum concentrator (Genevac Ltd., UK) for >2 h and gently resuspended in the running buffer (20 mM Hepes, 140 mM NaCl, pH 7.4) or sonicated, respectively. POPC sonicated liposomes were used as a negative control for the binding of ouabain. The POPC in chloroform was dried under pressure in a round-bottom flask to produce a thin lipid film. The running buffer used for the SPR measurements and glass beads were added to the flask and vortexed vigorously. The obtained lipid suspension was sonicated to produce SUVs, which were used for the binding assay. The SPR experiments were performed using a Biacore T100 instrument (GE Healthcare). The L1 sensor chip (GE Healthcare) was docked into the instrument and primed twice with the running buffer. Membrane preparations were diluted in the running buffer and injected over the surface of an L1 sensor chip at 2 μl/min. The capture level was kept between 900 and 1200 RU for all of them. The membrane surface was then allowed to stabilize for 420 s. To monitor the binding the ouabain was injected over the lipid surface in various concentrations (0, 2.5, 5, 10, and 20 mM). One concentration (5 mM) was repeated at the end of experiment to control the stability of the surface. The samples were injected for 1 min and dissociation was also monitored for the same period. Because of the fast dissociation no regeneration was needed between sample concentrations. The lipids were removed from the surface with three 30-s pulses of 40 mM octyl-β-d-glucopyranoside following one 30-s pulse of 0.5% SDS. The flow rate was set to 50 μl/min and all experiments were performed at 25 °C.

Results and discussion

GUVs prepared from erythrocyte membranes are a realistic model system that in principle mimics the intact plasma membrane, and thus it immediately attracted our attention. We accurately followed a previously described procedure (Table 1, protocol 1) [15] and succeeded in the preparation of GUVs from erythrocyte ghosts prepared in 150 mM NaCl, 20 mM Hepes, pH 7.4 (RBC–GUVs) (Figs. 1 and 2). However, we could not prepare sufficient amounts of large RBC–GUVs of uniform size for the functional studies. The average density of RBC–GUVs prepared in such a way was approximately six GUVs in 1 μl of a suspension (Fig. 1A, protocol 1). Moreover, RBC–GUVs were small with irregular shape; some of them frequently contained inclusions (Fig. 1B–D). For these reasons we aimed to improve the efficiency of electroformation to obtain higher amounts of large, spherical GUVs. We suspected that loss of water that evaporates from the ghosts during drying leads to higher osmolarity of the internal solution and, therefore, causes rupture of the nascent RBC–GUVs during the electroformation because of higher ionic strength in the interior compared to the surroundings. When we changed the buffer to pure water for the ghosts preparation (Table 1, protocol 2), the total number of RBC–GUVs, as well as the portion of spherical RBC–GUVs, markedly increased (Fig. 1A and C, protocol 2). To avoid the influence of the osmotic imbalance during the electroformation we prepared unsealed erythrocyte membranes in pure water (Table 1, protocol 3). To ensure firm attachment of lipid deposits on electrodes we dried lipid deposits at reduced pressure for a minimum of 2 h. The substitution of ghosts for the membrane did not significantly improve the electroformation efficiency (Fig. 1A and C, protocol 3). However, the advantage of this modification is that reproducible deposition of lipid membranes on the electrodes was achieved. The attachment of membrane deposits to the electrodes appears to be stronger compared to the ghost deposition, where we sometimes could not achieve firm attachment (data not shown). Next we changed the physiological buffer to water or sucrose in the electroformation step and used a low-frequency protocol for electroformation (Table 1, protocols 4 and 5). The presence of water during the electroformation step did not change the outcome of the GUV formation, while the presence of sucrose markedly increased the amount of RBC–GUVs gathered by one single electroformation, as well as the portion of spherical vesicles without inclusions (Fig. 1A and C). At first glance the presence of sucrose in the medium is a drawback since solutions containing a high amount of sugar are not an optimal environment for studying biological processes. Nevertheless, the sucrose solution can be later easily exchanged for physiologically more relevant buffer by slow pipetting as described in [13]. The presence of sucrose in the medium has three advantages. First, the RBC–GUVs with a dense sucrose interior will sink to the bottom and remain immovable, which is convenient during the microscopy. Second, the RBC–GUVs containing sucrose can also be further concentrated by adding iso-osmolar solution with lower density (e.g., glucose or buffer solution). Third, the RBC–GUVs prepared according to protocol 5 can be selectively concentrated to obtain a suspension of large RBC–GUVs. As the large GUVs sink faster they can be easily

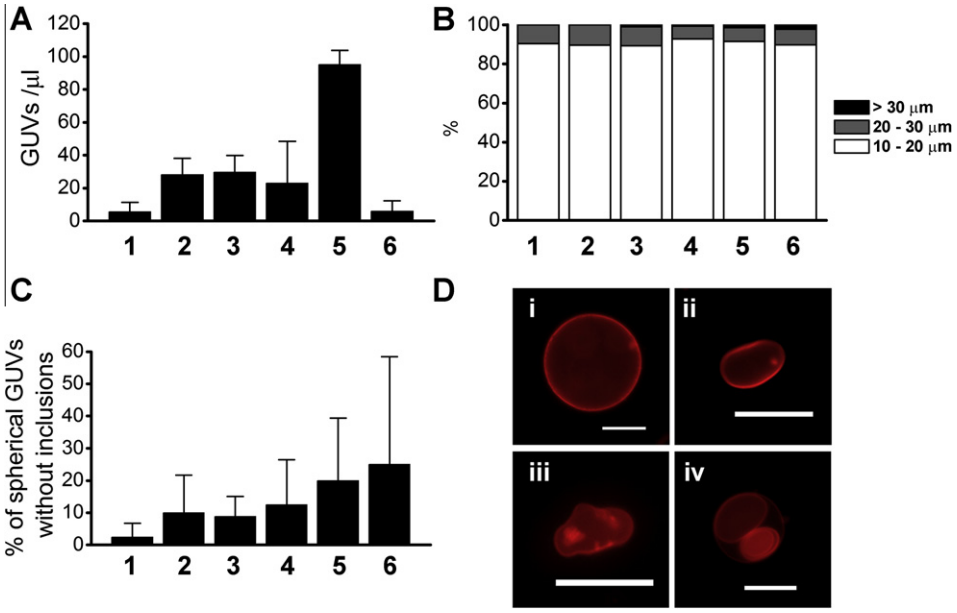

Fig.1. The efficiency of various protocols for electroformation. GUVs were prepared using the various protocols as described in Table 1 and observed by fluorescence microscope. Only GUVs larger than 10 µm were evaluated. (A) The amounts of GUVs prepared by protocols 1–6. Each column represents the average number of GUVs from three to five independent electroformations ± standard deviation. Altogether 84–2379 GUVs in 5 µl of suspension were evaluated for each electroformation protocol. (B) Size distribution of GUVs from three independent electroformations. Altogether 84–1346 GUVs in 5 µl of suspension were evaluated for each electroformation protocol. (C) The portion of spherical GUVs without inclusions. Each column represents the average percentage of GUVs from three independent electroformations ± standard deviation. Altogether 84–446 GUVs in 5 µl of suspension were evaluated for each electroformation protocol. (D) Representative images of the most recurrent GUV shapes: (i) spherical GUV, (ii) oval/oblong vesicle, (iii) irregular shape, (iv) GUVs with inclusion. GUVs contain $DiIC_{18}$ (red); scale bar, 20 µm. (For interpretation of the references to color in this figure legend, the reader is referred to the web version of this article.)

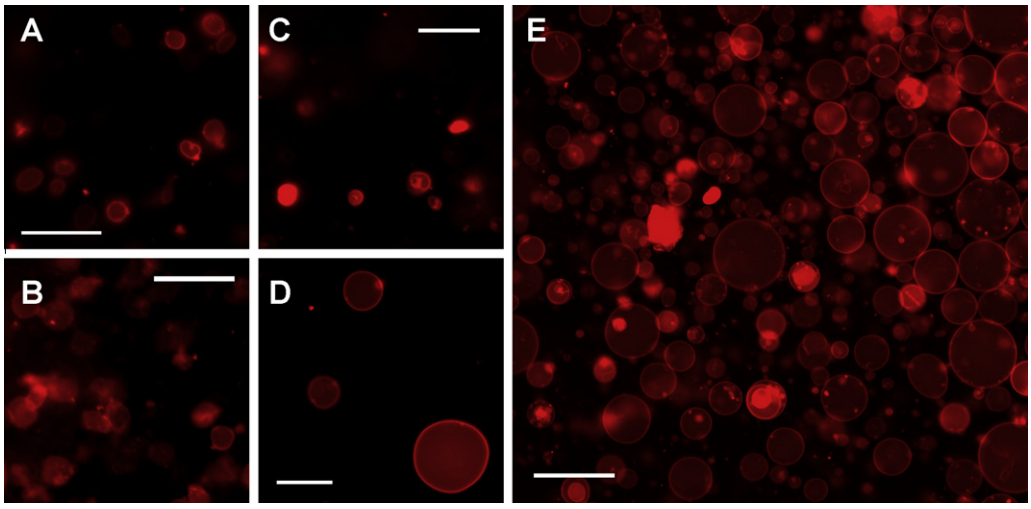

Fig.2. Fluorescent images of erythrocyte ghosts, membranes, and RBC–GUVs. (A) Erythrocyte ghosts, (B) membranes, (C) RBC–GUVs prepared by protocol 2, and (D) RBC–GUVs prepared by protocol 5. (E) Large RBC–GUVs prepared by protocol 5 contain sucrose and were sedimented by iso-osmolar buffer (150 mM NaCl, 20 mM Hepes, pH 7.4). Lipid membranes contain DilC18 (red); scale bar, (A–D) 20 µm, (E) 50 µm. (For interpretation of the references to color in this figure legend, the reader is referred to the web version of this article.)

collected in the first sedimentation fraction. In such a way we succeeded in preparing a suspension of extremely large RBC–GUVs as presented on Fig. 2E. We also checked how the volume of membranes deposited on the electrodes affects the electroformation efficiency (protocol 6). The amount of lipid deposited on the electrodes is clearly important, since we observed significantly lower amounts of RBC–GUVs formed when using 2 µl of membrane deposits (Fig. 1A). In addition, higher deposits of membranes, e.g., 32 µl, resulted in an even higher number of RBC–GUVs (data not shown). The majority of the RBC–GUVs prepared according to the described protocols measured <20 µm in diameter (Fig. 1B).

Next we wanted to compare the composition (lipids, proteins) of the RBC–GUVs prepared according to the improved protocol (protocol 5) with those prepared according to the procedure introduced by Montes et al. [15] (protocol 1). However, we did not succeed in preparing enough RBC–GUVs necessary for the lipid and protein analyses following protocol 1. Therefore we prepared the RBC–GUVs according to protocol 2, which is in principle the same protocol, differing only in the medium in which the ghosts are suspended (Table 1). To estimate the protein content and heterogeneity of the lipids in the membrane of RBC–GUVs, we measured the content of proteins by amido black reagents and the concentration

Table 2
Comparison of several membrane component concentrations in RBC–GUVs prepared by protocols 2 and 5

Electroformation protocol	Proteins (μg/ml)	Phospholipids (μg/ml)	Cholesterol (μg/ml)	Ratio (PL:CHO)
Protocol 2	19.9 ± 12.7	3.6 ± 2.2	1.4 ± 0.9	2.6:1
Protocol 5	11.7 ± 10.3	2.6 ± 2.0	1.0 ± 0.8	2.6:1

The values represent the average of three independent measurements ± standard deviation.

of phospholipids and cholesterol by enzymatic assays (Table 2). The mass ratio of phospholipids to cholesterol, 2.6:1 (Table 2), was practically identical for both procedures and it roughly corresponded to previously published data [24]. The concentration of all measured components (phospholipids, cholesterol, and proteins) was higher in suspensions of RBC–GUVs prepared according to protocol 2. The results are apparently contradictory to the counting experiments in which we counted approximately three times more RBC–GUVs in suspensions prepared according to protocol 5 (Fig. 1A). We suspect that this is due to the ghosts that fell off the electrodes during the electroformation according to protocol 2 and to the higher amount of smaller vesicles that were not evaluated in Fig. 1. In fact, we usually observed many small vesicles in suspensions of RBC–GUVs prepared according to protocols 1 and 2 (Fig. 2C).

One important aspect of studying GUVs from erythrocyte membranes is that they contain functional proteins. We have assessed the activity of some of the proteins associated with RBC membranes by enzymatic assays and SPR. We have found that the enzymatic activity of acetylcholinesterase [25] and phosphatase [26] that were associated with the RBC membranes, dried under the same conditions as were used for the preparation of GUVs and gently resuspended in the buffer, was comparable to that of the starting material. The sonication of the membranes led to the loss of enzymatic activity and this sample served us as a negative control (Fig. 3A). We also assayed GUVs prepared by protocol 1 and our protocol 5 for acetylcholinesterase activity and found both to be roughly comparable to the activity of red blood cell membranes that served as a starting material (Fig. 3A). As a complementary experiment we used the SPR to assess the binding of ouabain, an inhibitor of the Na^+–K^+-ATPase [27], and obtained a robust binding to membranes and dried membranes, but not to sonicated membranes or POPC liposomes that served as a negative control (Fig. 3B). The assays that we employed were not sensitive enough to assay produced GUVs; however, the results clearly indicate that the functionality of all three membrane proteins tested is retained after the drying we employed for the production of GUVs.

GUVs are an extensively used model system for investigating the permeabilization properties of pore-forming proteins [1,8] and peptides [28]. For this reason we tested the intrinsic permeability of the RBC–GUVs in the presence of various molecular weight probes. After 24 h incubation RBC–GUVs were virtually impermeable for a high-molecular-weight probe (dextran, 70 kDa) but approximately 35% of RBC–GUVs were permeable for a low-molecular-weight probe (calcein) (Fig. 4A and B). As expected GUVs prepared from synthetic lipid POPC remained impermeable to calcein influx after 24 h incubation (data not shown). These results indicate that the membrane of the RBC–GUVs is completely sealed up. In addition, integral membrane proteins, such as transmembrane channels, in a RBC–GUV membrane may be responsible for intrinsic permeability observed for calcein. Erythrocytes have several transmembrane channels, e.g., band 3 [29], potassium and sodium channels [30], aquaporin 1 [31], glucose transporter Glut1 [32], Ca^{2+} and Mg^{2+} ATPase [33], and several amino acid and nucleoside transporters [34]. Although the radius of the pores on erythrocyte membranes (3.5 to 4.2 Å) [35,36] is predicted to be slightly smaller than the hydrodynamic radius of calcein (~6 Å) [37], we suspect that they may allow the slow diffusion

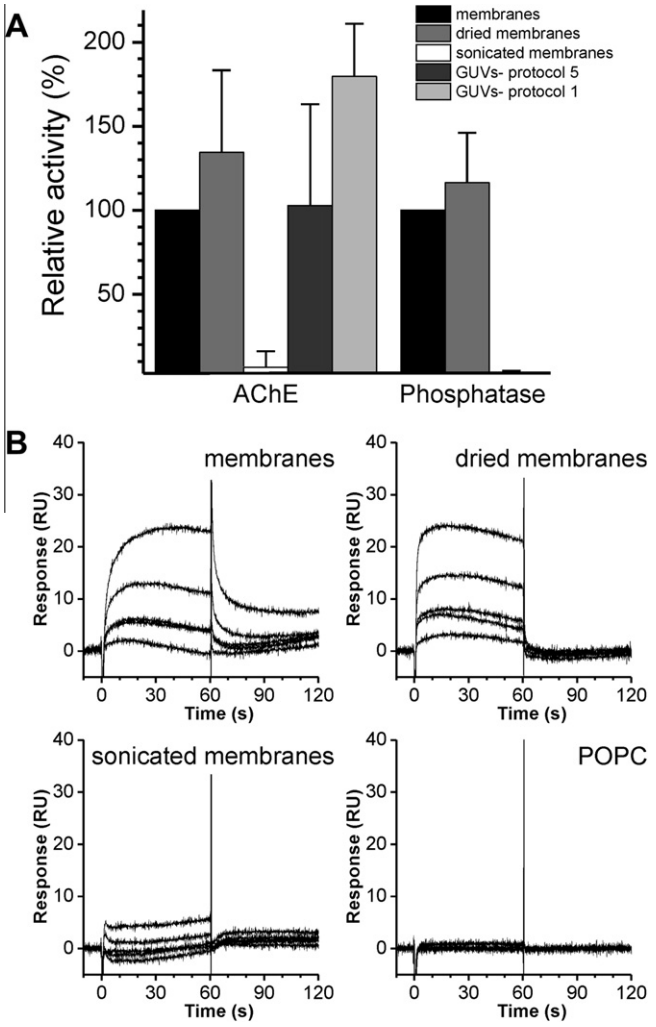

Fig.3. Functionality of proteins from RBC–GUVs assessed by enzymatic assays and SPR. (A) Relative enzymatic activity of AChE and K^+-(*p*-nitrophenyl phosphatase) in membranes, dried membranes, sonicated membranes, GUVs prepared using protocol 5, and GUVs prepared using protocol 1. Each column represents the average value of two to seven independent experiments ± standard deviation. Because of low sensitivity of the assay we could not measure the phosphatase activity for the GUV samples. (B) SPR analysis of ouabain binding to untreated membranes, dried membranes, sonicated membranes, and POPC SUVs. The concentrations used were 2.5, 5 (in replicate), 10, and 20 mM from the bottom to the top. Typical sensorgrams from three independent experiments are presented.

of calcein after prolonged incubation. The heterogeneity of the membrane proteins was confirmed by precipitating the proteins from the RBC–GUVs prepared according to protocol 5 and separating them by SDS–PAGE (data not shown). We searched for the presence of integral membrane proteins in the RBC–GUV by using specific antibodies against the extracellular domain of glycoprotein A. We confirmed the presence of this protein on the surface of RBC–GUVs, indicating that at least a proportion of this protein is in the expected orientation (Fig. 5A). We have also assessed the asymmetry of the membrane after the electroformation. Our preliminary results (not shown in this paper) indicate that the asymme-

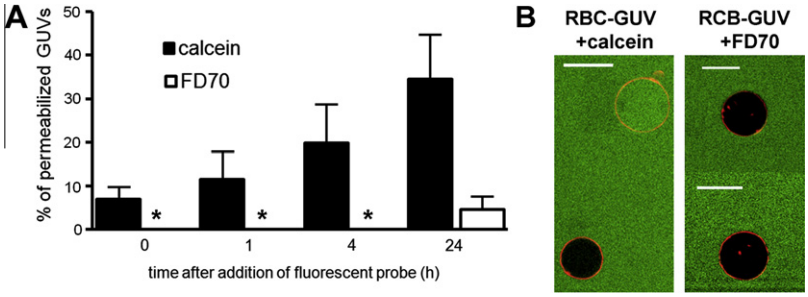

Fig.4. Intrinsic permeability of RBC–GUVs prepared using protocol 5. (A) RBC–GUVs prepared using protocol 5 were incubated in the presence of calcein or FD70 for 24 h. Each column represents the average value of three independent experiments ± standard deviation. We evaluated 135–218 GUVs. *Not measured. (B) Representative fluorescence microscopy images of RBC–GUVs in the presence of different fluorescent probes (green) after 24 h incubation. GUVs contain $DiIC_{18}$ (red); scale bar, 20 μm. (For interpretation of the references to color in this figure legend, the reader is referred to the web version of this article.)

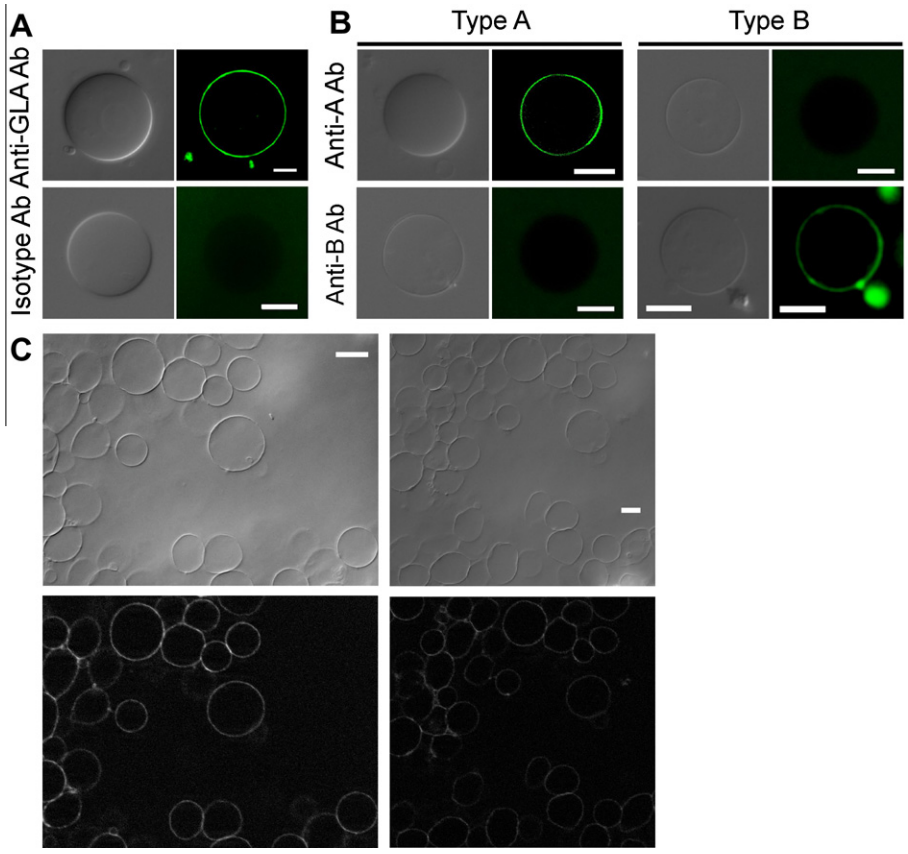

Fig.5. Staining of RBC–GUVs prepared using protocol 5. (A) Fluorescent images of glycophorin A on the surface of the RBC–GUVs detected by anti-glycophorin (GLA) Ab and isotype control. DIC images of GUVs are presented on the left and fluorescent images of the same GUV are shown on the right. (B) Fluorescent images of blood group antigens A (left) and B (right) on the surface of RBC–GUVs detected by anti-A and anti-B Ab. All RBC–GUVs were prepared using protocol 5. DIC images of GUVs are presented on the left and fluorescent images of the same GUV on the right. (C) Representative overview images of many GUVs prepared from a type B blood donor and stained with anti-B mAb. DIC images are shown above, fluorescent images are shown below. Scale bar, 10 μm.

try of the membrane lipids is not retained after electroformation, probably because of dehydration during drying that could destabilize the membrane bilayers and cause lipid mixing. Next we checked whether the RBC–GUVs in addition to proteins also contain membrane oligosaccharides characteristic of erythrocytes. Two particular membrane oligosaccharides were selected for the immunodetection: those of blood groups A and B (type A and type B oligosaccharides). We detected type A oligosaccharides only on RBC–GUVs prepared from blood group A and not on the RBC–GUVs prepared from blood group B and vice versa (Fig. 5B), which indicates that in addition to some membrane proteins the membrane oligosaccharides are also preserved on the membrane of the RBC–GUVs (protocol 5).

GUVs are usually prepared from well-defined mixtures of pure, mostly synthetic lipids. However, the resemblance of these model systems to actual biological membranes, which are much more complex mixtures of lipids, proteins, and saccharides, is questionable. Reconstitution of proteins into giant vesicles is still challenging because of technical problems in GUV preparation [38]. Many efforts were made in the past to compile the minimal experimental system resembling living cells. GUVs composed of native membranes seem promising candidates for the bottom-up approach toward the construction of a minimal cell. For all these reasons GUVs prepared from native membranes appear to be an ideal experimental system for studying various membrane-related phenomena [15]. In this paper we describe the protocol for GUV preparation

from remnants of red blood cells by introducing the following modifications: (i) we slightly changed the preparation of lipid deposits by using higher amounts of erythrocyte membranes in water instead of ghosts suspended in buffer, (ii) we increased the drying time to 2 h at reduced pressure to obtain lipid layers firmly attached to the electrodes, and (iii) we performed electroformation at low frequency in sucrose solution. These improvements enabled the high productivity of the formation of RBC–GUVs, similar to those prepared by synthetic lipids (e.g., POPC). The major advantage of the improved protocol is its high efficiency, since it produces ~20 times more RBC–GUVs over the published protocols (Fig. 1A). The analyses of membrane lipids, proteins, and oligosaccharides indicated that the native heterogeneity of those compounds in erythrocyte membranes is roughly preserved in RBC–GUVs. We have also shown that the activity of three membrane proteins that we used for testing was retained after employing the same drying conditions as used for preparation of RBC–GUVs (Fig. 3).

In addition to the evident advantages mentioned above there are several drawbacks of the improved protocol, mainly concerning the quality of the membranes in the GUVs. First, because of the conditions used for the preparation of GUVs it is not likely that the GUV membranes preserve the original lipid asymmetry. Furthermore, although we have shown protein activity for several proteins, others may be nonfunctional after the electroformation because of the drying step. Another potential drawback is the presence of sucrose in the electroformation buffer. However, this can also be an advantage in the case in which additional concentration of GUVs by sedimentation is needed (Fig. 2E). In summary, the protocol developed here enables preparation of large amounts of spherical GUVs with heterogeneous membrane composition that may be useful for functional studies of various membrane-related phenomena [39].

Acknowledgments

We thank the Slovenian Research Agency for support. We also thank Dr. Simon Koren for generously providing anti-A and anti-B antibodies.

References

[1] P. Schon, A.J. Garcia-Saez, P. Malovrh, K. Bacia, G. Anderluh, P. Schwille, Equinatoxin II permeabilizing activity depends on the presence of sphingomyelin and lipid phase coexistence, Biophys. J. 95 (2008) 691–698.
[2] M.M. Kozlov, Biophysics: joint effort bends membrane, Nature 463 (2010) 439–440.
[3] Y. Tamba, M. Yamazaki, Single giant unilamellar vesicle method reveals effect of antimicrobial peptide magainin 2 on membrane permeability, Biochemistry 44 (2005) 15823–15833.
[4] S. Nichols-Smith, S.Y. Teh, T.L. Kuhl, Thermodynamic and mechanical properties of model mitochondrial membranes, Biochim. Biophys. Acta 1663 (2004) 82–88.
[5] N. Khalifat, N. Puff, S. Bonneau, J.B. Fournier, M.I. Angelova, Membrane deformation under local pH gradient: mimicking mitochondrial cristae dynamics, Biophys. J. 95 (2008) 4924–4933.
[6] J. Majhenc, B. Bozic, S. Svetina, B. Zeks, Phospholipid membrane bending as assessed by the shape sequence of giant oblate phospholipid vesicles, Biochim. Biophys. Acta 1664 (2004) 257–266.
[7] A. Roux, D. Cuvelier, P. Nassoy, J. Prost, P. Bassereau, B. Goud, Role of curvature and phase transition in lipid sorting and fission of membrane tubules, EMBO J. 24 (2005) 1537–1545.
[8] T. Praper, A. Sonnen, G. Viero, A. Kladnik, C.J. Froelich, G. Anderluh, M. Dalla Serra, R.J. Gilbert, Human perforin employs different avenues to damage membranes, J. Biol. Chem. 286 (2011) 2946–2955.
[9] J.P. Reeves, R.M. Dowben, Formation and properties of thin-walled phospholipid vesicles, J. Cell. Physiol. 73 (1969) 49–60.
[10] A. Moscho, O. Orwar, D.T. Chiu, B.P. Modi, R.N. Zare, Rapid preparation of giant unilamellar vesicles, Proc. Natl. Acad. Sci. USA 93 (1996) 11443–11447.
[11] J.C. Stachowiak, D.L. Richmond, T.H. Li, A.P. Liu, S.H. Parekh, D.A. Fletcher, Unilamellar vesicle formation and encapsulation by microfluidic jetting, Proc. Natl. Acad. Sci. USA 105 (2008) 4697–4702.
[12] D.S. Dimitrov, M.I. Angelova, Lipid swelling and liposome formation mediated by electric-fields, Bioelectrochem. Bioenerg. 19 (1988) 323–336.
[13] D.J. Estes, M. Mayer, Giant liposomes in physiological buffer using electroformation in a flow chamber, Biochim. Biophys. Acta 1712 (2005) 152–160.
[14] H. Bouvrais, P. Meleard, T. Pott, K.J. Jensen, J. Brask, J.H. Ipsen, Softening of POPC membranes by magainin, Biophys. Chem. 137 (2008) 7–12.
[15] L.R. Montes, A. Alonso, F.M. Goni, L.A. Bagatolli, Giant unilamellar vesicles electroformed from native membranes and organic lipid mixtures under physiological conditions, Biophys. J. 93 (2007) 3548–3554.
[16] T. Pott, H. Bouvrais, P. Meleard, Giant unilamellar vesicle formation under physiologically relevant conditions, Chem. Phys. Lipids 154 (2008) 115–119.
[17] P. Peterlin, V. Arrigler, Electroformation in a flow chamber with solution exchange as a means of preparation of flaccid giant vesicles, Colloids Surf. B 64 (2008) 77–87.
[18] J.P. Goldring, L. Ravaioli, Solubilization of protein–dye complexes on nitrocellulose to quantify proteins spectrophotometrically, Anal. Biochem. 242 (1996) 197–201.
[19] G.L. Ellman, K.D. Courtney, V. Andres Jr., R.M. Feather-Stone, A new and rapid colorimetric determination of acetylcholinesterase activity, Biochem. Pharmacol. 7 (1961) 88–95.
[20] I. Mancini, A. Sicurelli, G. Guella, T. Turk, P. Maček, K. Sepčić, Synthesis and bioactivity of linear oligomers related to polymeric alkylpyridinium metabolites from the Mediterranean sponge *Reniera sarai*, Org. Biomol. Chem. 2 (2004) 1368–1375.
[21] V.L. Marcheselli, M.J. Rossowska, M.T. Domingo, P. Braquet, N.G. Bazan, Distinct platelet-activating factor binding sites in synaptic endings and in intracellular membranes of rat cerebral cortex, J. Biol. Chem. 265 (1990) 9140–9145.
[22] B. Bakrač, I. Gutierrez-Aguirre, Z. Podlesek, A.F. Sonnen, R.J. Gilbert, P. Maček, J.H. Lakey, G. Anderluh, Molecular determinants of sphingomyelin specificity of a eukaryotic pore-forming toxin, J. Biol. Chem. 283 (2008) 18665–18677.
[23] M. Beseničar, P. Maček, J.H. Lakey, G. Anderluh, Surface plasmon resonance in protein–membrane interactions, Chem. Phys. Lipids 141 (2006) 169–178.
[24] G. Salvioli, G. Rioli, R. Lugli, R. Salati, Membrane lipid composition of red blood cells in liver disease: regression of spur cell anaemia after infusion of polyunsaturated phosphatidylcholine, Gut 19 (1978) 844–850.
[25] J. Delaunay, The enzymes of the red blood cell plasma membrane, Biomedicine 26 (1977) 357–361.
[26] P.J. Garrahan, M.I. Pouchan, A.F. Rega, Potassium activated phosphatase from human red blood cells: the mechanism of potassium activation, J. Physiol. 202 (1969) 305–327.
[27] J. Wang, J.B. Velotta, A.A. McDonough, R.A. Farley, All human Na^+–K^+-ATPase alpha-subunit isoforms have a similar affinity for cardiac glycosides, Am. J. Physiol. Cell. Physiol. 281 (2001) C1336–C1343.
[28] E.E. Ambroggio, F. Separovic, J.H. Bowie, G.D. Fidelio, L.A. Bagatolli, Direct visualization of membrane leakage induced by the antibiotic peptides: maculatin, citropin, and aurein, Biophys. J. 89 (2005) 1874–1881.
[29] A.H. Ross, H.M. McConnell, Reconstitution of band 3, the erythrocyte anion exchange protein, Biochem. Biophys. Res. Commun. 74 (1977) 1318–1325.
[30] C. Brugnara, Membrane transport of Na and K and cell dehydration in sickle erythrocytes, Experientia 49 (1993) 100–109.
[31] B.M. Denker, B.L. Smith, F.P. Kuhajda, P. Agre, Identification, purification, and partial characterization of a novel Mr 28,000 integral membrane protein from erythrocytes and renal tubules, J. Biol. Chem. 263 (1988) 15634–15642.
[32] M. Mueckler, Facilitative glucose transporters, Eur. J. Biochem. 219 (1994) 713–725.
[33] D.M. Waisman, J.M. Gimble, D.B. Goodman, H. Rasmussen, Studies of the Ca^{2+} transport mechanism of human erythrocyte inside-out plasma membrane vesicles. I. Regulation of the Ca^{2+} pump by calmodulin, J. Biol. Chem. 256 (1981) 409–414.
[34] J.C. Ellory, J.D. Young, Neutral amino acid transport in erythrocytes from different mammalian species, J. Physiol. 272 (1977) 43P–44P.
[35] D.A. Goldstein, A.K. Solomon, Determination of equivalent pore radius for human red cells by osmotic pressure measurement, J. Gen. Physiol. 44 (1960) 1–17.
[36] K. Kinosita Jr., T.Y. Tsong, Formation and resealing of pores of controlled sizes in human erythrocyte membrane, Nature 268 (1977) 438–441.
[37] M.R. Prausnitz, J.D. Corbett, J.A. Gimm, D.E. Golan, R. Langer, J.C. Weaver, Millisecond measurement of transport during and after an electroporation pulse, Biophys. J. 68 (1995) 1864–1870.
[38] Y.H. Chan, S.G. Boxer, Model membrane systems and their applications, Curr. Opin. Chem. Biol. 11 (2007) 581–587.
[39] T. Praper, A.F. Sonnen, A. Kladnik, A.O. Andrighetti, G. Viero, K.J. Morris, E. Volpi, L. Lunelli, M. Dalla Serra, C.J. Froelich, R.J. Gilbert, G. Anderluh, Perforin activity at membranes leads to invaginations and vesicle formation, Proc. Natl. Acad. Sci. USA 108 (2011) 21016–21021.